Is the functional response of a receptor determined by the thermodynamics of ligand binding?

Martin Vögele[1], Bin W. Zhang[1], Jonas Kaindl[2], Lingle Wang[1,*]

[1] Schrödinger, Inc., 1540 Broadway 24th Floor, New York, NY 10036, United States.
[2] Schrödinger GmbH, Glücksteinallee 25, 68163 Mannheim, Germany.
*Email: lingle.wang@schrodinger.com; Phone: +1 (212) 548-2381

ABSTRACT

For an effective drug, strong binding to the target protein is a prerequisite but it is not enough. To produce a particular functional response, drugs need to either block the proteins' functions or modulate their activities by changing the conformational equilibrium. The binding free energy of a compound to its target is routinely

calculated but the time scales for the protein conformational changes are prohibitively long to be efficiently modeled via physics-based simulations. Thermodynamic principles suggest that binding free energies of the ligands with different receptor conformations may infer their efficacy. However, this hypothesis has not been thoroughly validated. We present an actionable protocol and a comprehensive study to show that binding thermodynamics provides a strong predictor for the efficacy of a ligand. We apply the absolute-binding free energy perturbation (ABFEP) method to ligands bound to active and inactive states of eight G protein–coupled receptors and a nuclear receptor, then compare the resulting binding free energies. We find that carefully designed restraints are often necessary to efficiently model the corresponding conformational ensembles for each state. Our method achieves unprecedented performance in classifying ligands as agonists or antagonists across the various investigated receptors, all of which are important drug targets.
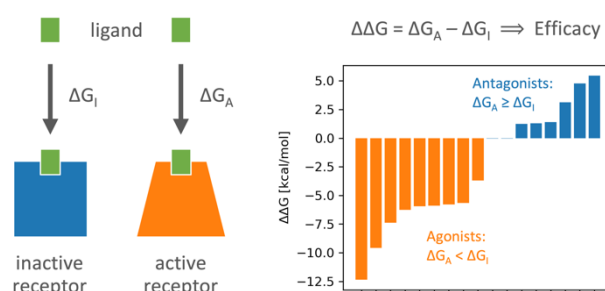
INTRODUCTION

Small molecule drugs achieve their therapeutic effects by binding to specific sites on larger biomolecules such as enzymes or receptors and triggering functional responses in their targets. The simplest functional response is steric inhibition where binding affinity is often sufficient to describe the effect. More complex effects require the ligand to alter the conformational ensemble of the target. These effects include triggering receptor activation, i. e., switching the receptor from an inactive to an active state,[1–5] and altering activation in a specific way such as allosteric modulation[6,7] or biased signaling.[8] The selective activation of certain targets within a protein subfamily can be attributed to either differences in binding affinity or differences in the resulting effects.[9] Consequently, while knowing the binding affinity of a ligand is crucial, it is often not sufficient to understand its full effect. Assessing a ligand's efficacy, its influence on the thermodynamic equilibrium between conformational states of the target, is equally important.

In drug discovery, the routine process of calculating binding free energy (affinity) contrasts with the more challenging task of examining ligand efficacy. Both ligand binding and transitions between multiple conformational states occur on timescales that typically surpass the capabilities of classical molecular dynamics (MD) simulations. While efficient end-point methods including free energy perturbation (FEP)[10–12] have been developed for accurate binding free energy calculations, the complex reorganization mechanisms for receptor activation make the corresponding pathways extremely difficult to model even with sophisticated enhanced-sampling methods.[13–15]

Fortunately, the multiple conformations of the receptor relevant to its activation may be linked with ligand binding via a thermodynamic model (Fig. 1). The thermodynamic cycle for a ligand binding to a two-state receptor responsible for its activation (Fig. 1B) implies that the difference in binding free energy of the ligand between the two receptor states might serve as a substitute for the receptor reorganization free energy. The effect of a ligand on the receptor can be described by how the free energy difference between the active and inactive state changes upon ligand binding from ΔG_{apo} to ΔG_{holo}. According to the thermodynamic model, this change $\Delta\Delta G = G_{holo} - \Delta G_{apo}$ is equivalent to the difference between the binding free energies of the ligand to each state: $\Delta\Delta G = \Delta G_A - \Delta G_I$. Note that the absolute values of ΔG_{apo} and ΔG_{holo} are not necessary to characterize the ligand's effect on the target, only the relative difference in the presence of the ligand as compared to in its absence. Thus, assuming that the distribution among the receptor conformations responsible for its activation is determined by thermodynamics, the functional efficacy of the ligand may be accurately modeled by the binding free energy calculations. For example, favorable binding to the active state over the inactive state ($\Delta G_A < \Delta G_I$) implies that a ligand is an agonist. This relation can be generalized to receptors with an ensemble of active or inactive conformations given knowledge of a receptor's underlying conformational space. The few studies that have applied this principle in the past to explain the functional responses of ligands provide encouraging, albeit anecdotal, evidence for its applicability. Saleh et al. compared the ligand

2

binding free energy calculated via metadynamics on different states of the receptor to explain biased signaling of the β2-adrenoceptor.[16] An analogous version of this thermodynamic model for relative binding free energies has recently been used to design partial agonists for the same target[17] and for the adenosine receptor A2A.[18] Similarly, the docking scores of ligands in distinct conformational states were used as a proxy for the binding free energy to predict the functional responses of various ligands.[19–21] The ATOM3D benchmark study proposed the use of structure-based machine-learning (ML) models for ligand efficacy prediction (LEP) following the same hypothesis.[22]

Despite these interesting attempts, this paradigm has not been adopted in practical drug discovery. Its general viability is still questionable due to a lack of systematic validation across targets and discouraging results from some of the related methods. For example, neither docking scores nor the best structure-based ML methods in the ATOM3D LEP benchmark reached acceptable general accuracy.[22] It has yet been unclear whether these methods fail due to the static nature of their model or due to faults in the thermodynamic rationale. In particular, the kinetics of ligand binding and of protein conformational changes, which depends on the free energy barriers along the respective pathways, can complicate efficacy prediction.[23–28] The lack of relevant structures for the active and inactive receptor conformations also made it difficult to validate the above paradigm, as typical drug-discovery workflows still focus on binding affinities to a single structure, and having experimental structures of a target in multiple conformational states available was a rare luxury until quite recently.

We demonstrate that the shift in free energy differences between receptor conformational states is the dominant factor that determines ligand efficacy and present an actionable strategy to predict it. We develop and validate a workflow for calculating this shift between the active and inactive states of G protein-coupled receptors (GPCRs) and nuclear receptors (NRs), two important classes of drug targets.[29,30] Our findings show that the free energy shift accurately predicts whether a ligand is an agonist or antagonist. Additionally, we discuss the prerequisites, strengths, and limitations of the proposed protocol to facilitate its use in drug discovery.

RESULTS

General Performance

We calculated the difference of binding free energies to the inactive state and the active state using absolute binding FEP (ABFEP),[12] which enables us to separate agonists from antagonists with high accuracy (Figure 2). Out of 180 target-ligand pairs, 168 were predicted correctly from the binding free energy difference ($\Delta\Delta G$) using a classification threshold of zero, resulting in an overall accuracy of 93%. The accuracy can be further improved to 98% when the threshold for classification is tuned for each receptor, with only three misclassified compounds. Small deviations of the optimal value of the threshold for classification from the theoretical zero reflect that ligands with negligible but favorable interactions with the active conformations of the

receptors can still be seen as (neutral) antagonists. Larger deviations for some systems suggest a possible systematic shift in the absolute binding free energy calculations for one of the receptor states. This will not affect the prospective predictions in practical applications if the optimal threshold value is calibrated accordingly. We also attempted to separate agonists from antagonists based on the ligand binding free energies with one of the receptor states (ΔG_A, or ΔG_I). None of them was able to consistently obtain a classification accuracy comparable to what is obtained via $\Delta\Delta G$ (Supporting Information Table S1), indicating that the functional response of the receptor is determined by the balance between the receptor conformational states, not by the free energy of a single state.

β-Adrenoceptors

We used the well-studied adrenoceptors β_1 and β_2 to develop our protocol, particularly focusing on finding suitable restraints that effectively separate active and inactive states while preserving conformational flexibility within each state (Figure 3A and 3B). To prevent ligands from inducing changes in the binding pocket towards their own preferred state, as opposed to the state being probed (Figure 3A), we applied flat-bottom harmonic restraints on the Cα atoms of the protein during the ABFEP simulations (Figure 3B, for details see the methods section). A comparison between simulations with and without these restraints (Figure 3C) revealed a significant accuracy gain when using the restraints, confirming the validity of our underlying reasoning. Notably, the restraints ensured that the separation between agonists and antagonists was close to $\Delta\Delta G = 0$, an outcome that had not been achieved by similar approaches in previous studies with tight restraints outside the binding pocket.[17,18] Overall, our protocol has proven effective in accurately separating agonists and antagonists.

Adenosine Receptors

The results on adenosine receptors corroborate the findings from our protocol's development. We observed good performance on both A1 and A2A receptors, with only one outlier in A2A. A particularly encouraging example is the correct prediction of the efficacy of the hybrid ligand LJ-4517 (Figure 4B) which features one functional group typical for agonists and another one typical for antagonists — an intuitively difficult to predict combination. Analysis of the only misclassified ligand LUF8852 on the A2A receptor (Figure 4D) revealed a limitation of the current model: if the ligand induces a receptor conformation that is very different from the template used in the simulations and that cannot be sampled in the relatively short ABFEP simulations, the current method may not accurately model that ligand. In this case, LUF8852's native experimental structure differs substantially from both template structures, and these structural changes were not sampled in the simulations, leading to the misclassification.

It should be noted that accurate ligand poses are critically important to classification. For the A1 receptor from the LEP dataset included in the ATOM3D machine-learning benchmark, our ABFEP workflow applied to the naively docked poses provided with the benchmark achieved an AUC-

ROC of 0.84 and an accuracy of 80%, a significant improvement over the state-of-the-art method for this target (AUC-ROC: 0.56, accuracy: 53%). However, we obtained even higher performance by running ABFEP on improved ligand poses — from docking guided by alignment to the maximum common substructure (MCS) of a known ligand pose — which yielded an AUC-ROC of 0.96 and an accuracy of 87% (see Supplementary Information Figure S2).

Opioid Receptors

We successfully achieved accurate predictions for a congeneric series of morphine-like opioids, despite the inherent challenges associated with this class of compounds. Chemically similar opioids can exhibit different functional responses, so-called activity cliffs (Figure 4A and Supplementary Information Figure S3), making efficacy prediction particularly difficult. Nevertheless, our approach yielded perfect prediction results for the δ-opioid receptor (δ-OR) and only one incorrect prediction for the μ-opioid receptor. When ABFEP calculations on the δ-OR were performed with restraints corresponding to its experimental structures instead of those derived from MD simulations, we observed a decrease in accuracy from 100% to 79% (Figure 3D). We attribute this decline to artifacts stemming from crystal packing, which are resolved in the template MD simulations (see Supporting Information Figure S4).

Serotonin Receptors

We extended our validation study to serotonin receptors, examining ligands with multiple scaffolds (see Figure 4C for examples). In this case, two ligands for receptor 1B and three for receptor 2A would be misclassified with the theoretical $\Delta\Delta G$ threshold of 0 for the binding free energy difference. Most of the misclassifications will be remediated by adjusting the threshold, leaving only one outlier. The relatively large threshold shift observed in receptor 2A is likely due to unmodeled missing loops in these simulations.

Retinoic Acid Receptor α

To investigate the validity of our approach beyond GPCRs, we classified a set of ligands for the retinoic acid receptor α (RAR-α), a nuclear receptor and — in contrast to the membrane-bound GPCRs — a soluble protein. Even without using restraints, ABFEP perfectly separated agonists and antagonists, with only one antagonist's predicted $\Delta\Delta G$ slightly below the theoretical threshold of 0 (Figure 2I). This result suggests that the thermodynamic principles we assume are applicable across multiple classes of drug targets.

DISCUSSION

Our results provide strong evidence for the thermodynamic theory that underpins our approach: the primary determinant of ligand efficacy is the thermodynamics of its binding. The difference in free energies is mostly adequate for estimating a ligand's overall efficacy. Simulating the entire

5

reorganization of a protein for each ligand is not necessary. Neglecting binding and unbinding kinetics does not preclude predicting a ligand's agonism, implying that kinetics is a secondary factor that may affect efficacy in a quantitative rather than qualitative way. It is important to note, however, that ligand efficacy is distinct from drug efficacy, which also depends on the cellular context.

We demonstrate the technical feasibility of accurately predicting ligand efficacy using ABFEP on various states of the target. Our method can be applied to sufficiently resolved targets with currently available software and force field parameters. Additionally, we demonstrate that ABFEP by far outperformed the comparison of docking scores, which in turn outperformed all current structure-based ML models.[22] This success highlights the advantages of physical modeling in small-data regimes as we can attribute it both to the ability to refine the experimental structures and to the explicit modeling of entropic contributions and the dynamic character of molecular systems. In particular, our method performs well for activity cliffs between similar ligands and can extrapolate into unknown chemical space. This extrapolation to new scaffolds is made possible by the use of ABFEP which, in contrast to relative-binding FEP (RBFEP), does not require knowing the binding affinity of a congeneric ligand. It enables efficacy prediction during the hit discovery stage of drug development where diverse scaffolds need to be evaluated.[31,32] The efficiency of the calculations can be improved in large-scale screenings via the combination of using ABFEP for a few representative ligands and RBFEP for compounds that are congeneric to those, followed by ML models trained on ligands scored by free energy calculations. In this context, we expect efficacy prediction via FEP to play an important role in many drug discovery campaigns.

The main requirements for practical applications of the method are good sampling of template ensembles and accurate ligand poses. While it is preferable to have at least one experimental template structure for each state, the various conformational states can in principle be obtained by enhanced-sampling simulations,[15,33] homology modeling,[34] or AlphaFold2[35–39] in combination with appropriate refinement.[40] Determining the dynamics within each state via MD simulations is usually straightforward. In cases where multiple conformations exist for the same activation state of the receptor (LUF5833 example in Figure 4D), sampling could be improved by using multiple active structures or multiple inactive structures, respectively, for the same target if available. As we gain more understanding of how receptors' conformational ensembles influence the details of ligand efficacy,[41,42] we anticipate that our method can be applied to resolve distinct sub-states of the active macrostate and thus to classify the different activation pathways in a similar fashion as we have shown for the distinction between agonism and antagonism.

We translate the knowledge about the structure-function relationship to our FEP calculations via restraints that ensure a clear distinction between the relevant states (here: active vs inactive) whenever the conformational ensembles otherwise tend to be similar or even overlap. We found that restraining the backbone Cα-atoms using a flat-bottom harmonic potential allows for enough flexibility to accurately represent entropic contributions to the free energy. The subtler the

6

differences in the receptor ensemble between various functional responses are, the more careful these restraints must be set up.

A good ligand pose is crucial as a general prerequisite for FEP calculations. This is not an issue in most lead optimization projects as the crystal structure of the lead compound is usually available at this stage. For uncertain poses that arise in more explorative projects, ABFEP can be combined with a pose-prediction algorithm such as induced fit docking molecular dynamics (IFD-MD).[43,44] In this case, FEP can also be used to refine the ranking of various candidate poses. These requirements are met in many projects where the use of binding free energy methods can be beneficial to estimate ligand efficacy.

In conclusion, we demonstrate that the thermodynamics of ligand binding is the primary determinant of ligand efficacy, and that the difference in the binding free energies between the ligand with the various activation states of the receptor is sufficient for estimating a ligand's overall efficacy. The approach we present can be applied to many targets with state-of-the-art simulation methods and its excellent accuracy by far outperforms docking scores and ML models. Through in-depth discussions of template structures, restraints, and poses, we highlight the key factors and limitations for practical application. Our findings have significant implications for the drug discovery process as they allow detailed predictions of a ligand's effects on its target.

METHODS

Data Curation.

We predicted ligand efficacy for 180 target-ligand pairs using ABFEP with restraints to template ensembles derived from MD simulations. We chose mostly GPCRs as our validation systems because they are the most important class of drug targets, with numerous structures available for study.[29,30] Additionally, we investigated a nuclear receptor, representing another important target class. Ligands were chosen from compounds with available functional data, mostly from the IUPhar/BPS Guide to Pharmacology Database,[45] such that they include congeneric series (morphinan opioids) but also a variety of scaffolds for the same targets (serotonin receptor ligands). For lists of all compounds with corresponding results, see the Supporting Information.

Molecular Dynamics Simulations.

For each target, we obtained template conformational ensembles from unbiased MD simulations, initiated from at least one active experimental structure with the receptor bound to an agonist and one inactive experimental structure with the receptor bound to an antagonist. We used the trajectories from these MD simulations to derive starting structure and, where necessary, restraints for the subsequent FEP calculations, following a systematic approach to quantify different structural ensembles[46] (Supporting Information Text and Figure S5). We computed distances between the Cα atoms of residues in the binding pocket and conducted k-means clustering in their

7

joint principal-component space. We calculated average positions within each cluster for all the receptor's Cα atoms to use them as restraint centers, and the RMSF for each cluster to use it as the width of the restraints. Where necessary, we rescaled this width to prevent overlap between active and inactive states. For simulation parameters and details on setup and analysis, see the Supporting Information.

Absolute Binding Free Energy Perturbation.

For each target-ligand pair, we performed ABFEP using FEP+.[10–12,47] This implementation uses replica exchange with solute scaling (REST2)[48] to improve sampling of the solute and Grand Canonical Monte Carlo (GCMC)[49] to enhance sampling of water molecules. To avoid artifacts in long-range electrostatic interactions for charged ligands,[50] it employs the alchemical water approach.[12,51] As the starting structure, we chose a frame from the template simulation in which the target had sufficiently relaxed. Ligands with available PDB structures were placed by aligning the structures at the receptor, congeneric ligands by aligning the ligands themselves, and poses for the additional benchmark study were generated using maximum common substructure (MCS) docking in Glide.[52,53] Restraints were applied using a flat-bottom harmonic potential on the receptor's Cα-atoms (Figure 3B) with their centers and widths determined from the template simulations as described above. We analyzed the results using custom Python scripts. Plots were generated using Matplotlib,[54] protein visualizations using PyMOL,[55] and chemical structures using Maestro's 2D Sketcher.[56]

Data and Software Availability.

The FEP+ program with OPLS4 force field in Schrödinger's 2023-1 release used to generate the data reported in the manuscript is available via standard commercial or evaluation licenses. Our workflow to analyze template MD simulations and set up restrained ABFEP calculations is available on GitHub at https://github.com/schrodinger/fep-restraints. FEP starting structures, results, and code for functional response predictions from free energies are available on GitHub at https://github.com/schrodinger/functional-response.
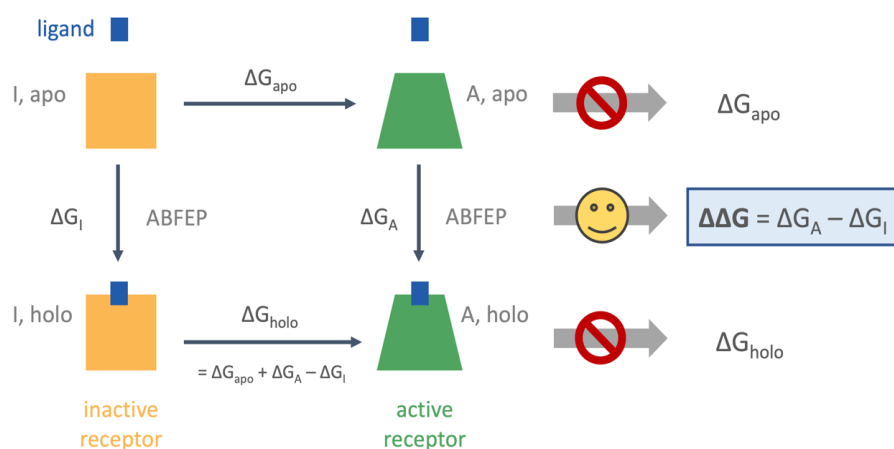
FIGURES

**A** Ligands shift the structural equilibrium between active and inactive state.
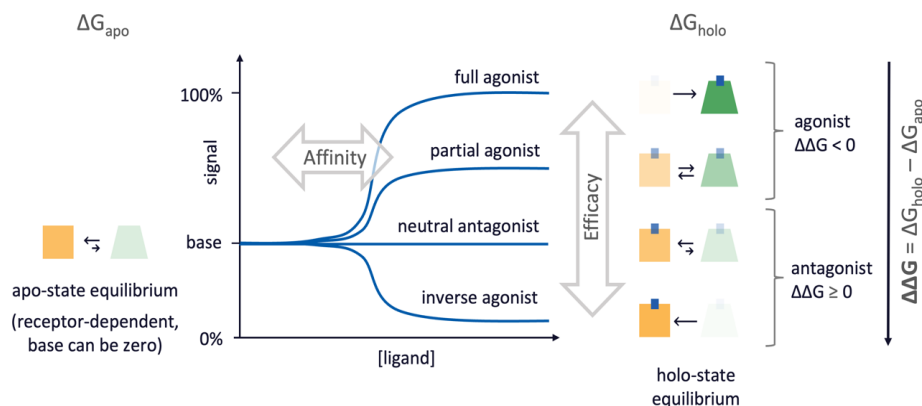
**B** The shift can be calculated via the binding free energies to each state.

Figure 1. The effect of a ligand on the structural equilibrium of a receptor can be predicted by comparing its binding affinity to the receptor in each relevant state.

(A) Thermodynamic equilibrium between the active state and the inactive state in a two-state receptor. The behavior of four types of ligands is shown: a full agonist, a partial agonist, a neutral antagonist, and an inverse agonist. In our analysis, the former two are categorized simply as agonists and the latter two as antagonists. The curves illustrate the typical downstream signal behavior over the ligand concentration for each type of ligand. The schematics represent the populations of active and inactive states in the apo and holo ensembles of the receptor in complex with the various ligand types, respectively. The difference in free energy between active and inactive states is called ΔG_{apo} in the apo ensemble and ΔG_{holo} in the holo ensemble. **(B)** The thermodynamic cycle of a two-state receptor, suggesting that the shift $\Delta\Delta G$ in the active-vs.-inactive equilibrium caused by a ligand can alternatively be calculated as the difference of the binding free energies ΔG_A and ΔG_I. Usually, obtaining ΔG_{apo} and ΔG_{holo} from conformational transitions of the receptor is prohibitively expensive (crossed arrows) but the binding free energies ΔG_A and ΔG_I are routinely calculated via established FEP methods (arrow with smiley face). While efficacy and affinity are orthogonal quantities, they are linked via thermodynamics. This relationship provides a useful "shortcut" for drug discovery and receptor biology and can be generalized to multi-state systems.
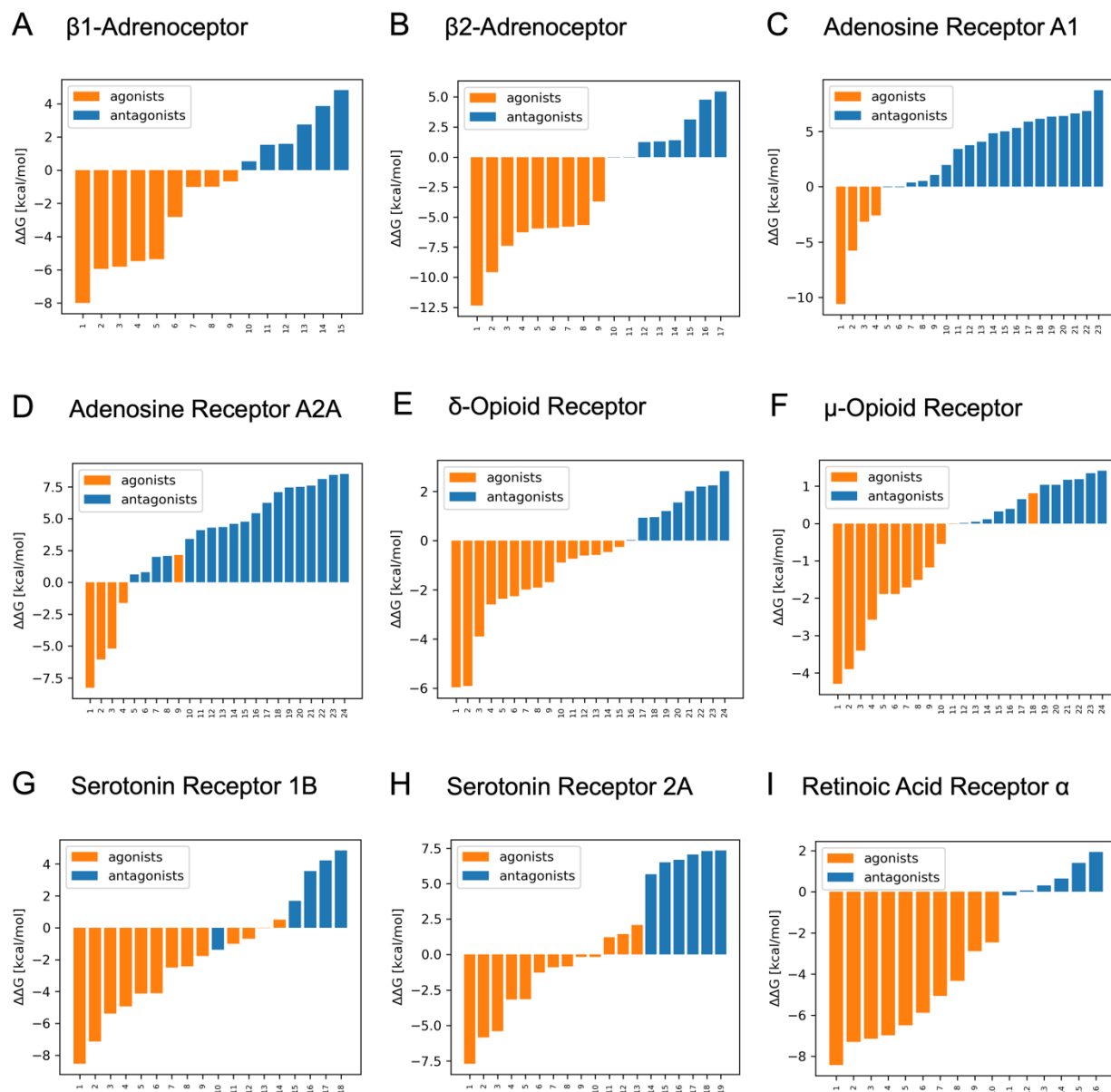
Figure 2. The difference of binding free energies calculated with FEP+ predicts the experimentally determined ligand efficacy with high accuracy across a large set of important receptors.

Each panel (A-H) shows the predicted shift ΔΔG from the inactive to the active state caused by each ligand for one of the target receptors in our study. The height of the bars indicates the predicted efficacy, with values expected to be lower for agonists (orange bars) and higher for antagonists (blue bars). Ligands are enumerated along the x-axis. A list of all ligand names and more detailed results can be found in the Supporting Information. Our findings demonstrate the utility of binding free energy calculations in predicting ligand efficacy.

10
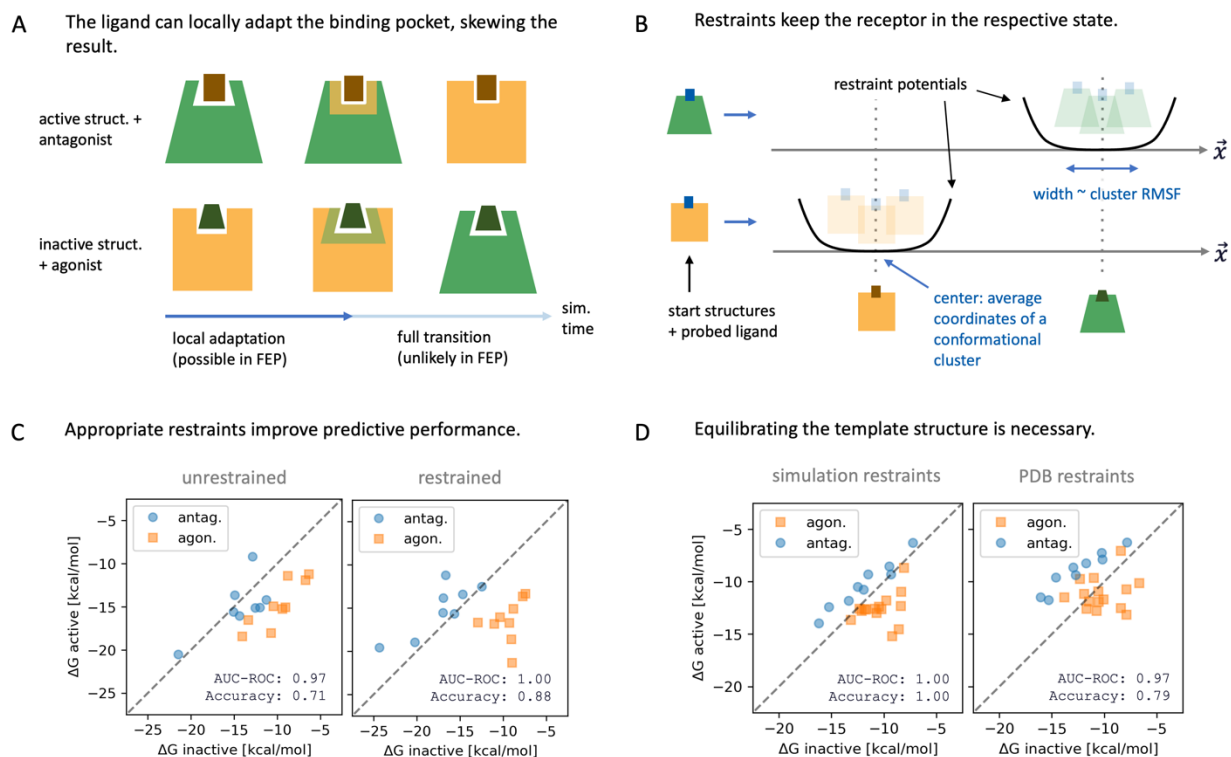
Figure 3. The predictive power of binding free energy calculations is strongly influenced by the separation between active and inactive conformational ensembles in FEP simulations.

(A) Ligands may prefer binding to a receptor in a conformational state other than the active or inactive state, as shown in the schematic representation of ligands (antagonist: brown rectangle, agonist: dark green trapezoid) and receptor conformations (first column). Without restraints, ligands can adapt the receptor to their preferred state (third column) via initial binding pocket accommodation (second column). **(B)** To improve predictive accuracy, flat-bottom harmonic restraints were applied to maintain the receptor in either the inactive or active state (left and right, respectively). The restraint centers and widths were determined from template MD simulations as described in the methods section. **(C)** A comparison of efficacy predictions from ABFEP with and without restraints is shown in scatter plots of binding free energies to the inactive and active states. Antagonists (blue circles) are expected to be at the top left and agonists (orange circles) at the bottom right. The improvement in predictive performance demonstrates the improvement from the use of restraints. **(D)** The comparison of efficacy predictions using restraints derived from MD simulations and those using restraints derived from the unrelaxed PDB structure (with slight distortions from crystal contacts) show that the best restraint center is not necessarily the experimental structure. While restraints from MD simulations lead to accurate predictions, strong-binding ligands (lower left) are consistently shifted upwards in the scatter plot obtained using the PDB structure-based restraints, indicating imperfect binding to the active structure. We explain this effect by slight distortions of the active experimental structure (PDB: 6PT2) from crystal contacts that are remedied during the template simulations (Supporting Information Figure S4).

11
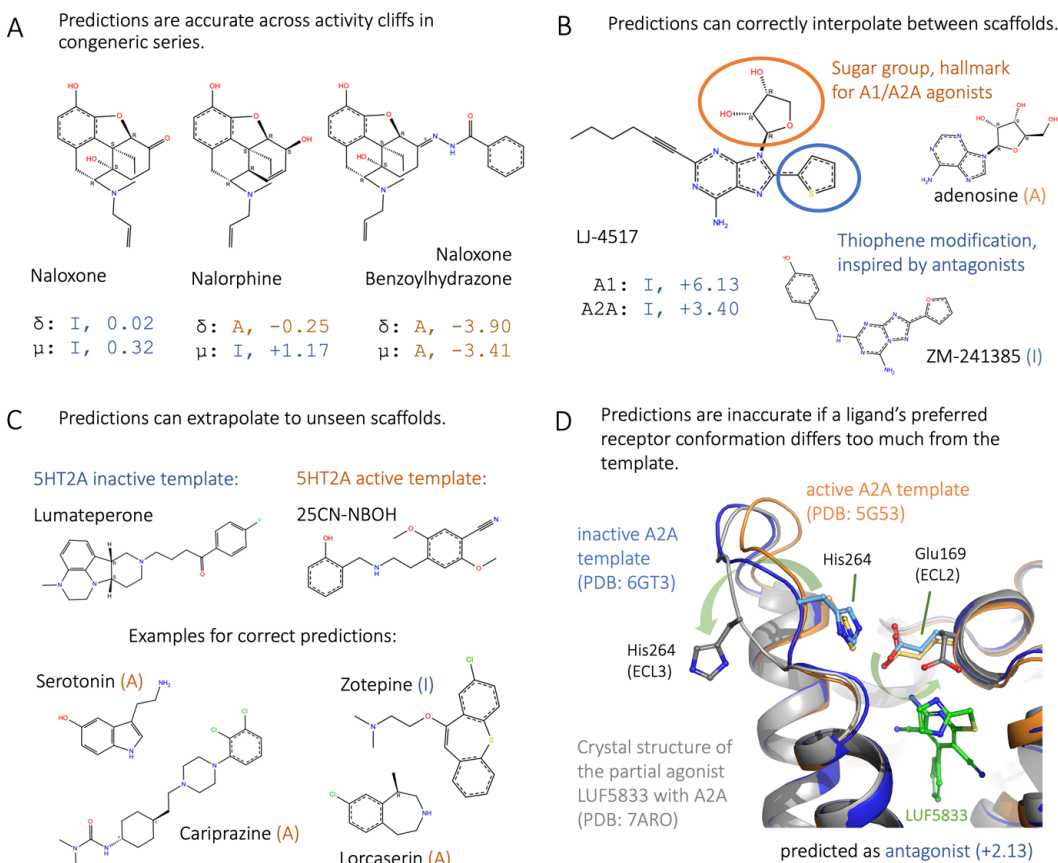
Figure 4. Our workflow can accurately predict functional responses of ligands across chemical space — including activity cliffs, scaffold interpolation and extrapolation — within the range of receptor conformations sampled by the template MD simulations.

(A) Three morphine-like opioids with subtle chemical differences and distinct functional responses at the δ- and μ-opioid receptors. Our workflow correctly predicts these differences, despite the "activity cliff" and the contrasting trends between the two receptors. Each ligand is labeled with its name and, for each of the two investigated opioid receptors, its experimentally determined efficacy (I: antagonist, A: agonist), and the value of the free energy shift ΔΔG in kcal/mol as predicted from ABFEP. **(B)** The "hybrid" ligand LJ-4517 contains functional groups associated with both adenosine receptor agonists (orange circle) and antagonists (blue circle), making its functional response difficult to predict from its structure alone. Our workflow correctly predicts it as an adenosine receptor antagonist. For comparison, we show the native agonist adenosine and the prototypical antagonist ZM-241385. **(C)** The ligands used in the template MD simulations for the serotonin receptor 2A (5HT2A), along with examples of probed ligands whose functional responses (I: antagonist, A: agonist) were correctly predicted. Note the diversity of scaffolds among these examples and compared to the template ligands. **(D)** LUF5833 was predicted as an A2A antagonist, contrary to its actual behavior as a partial agonist. This discrepancy can be attributed to the conformational changes in the receptor binding pocket, as observed in its experimental structure (PDB: 7ARO, gray) which was not used in our simulations. The binding pocket conformation differs significantly from both the active (5G53, orange) and inactive (6GT3, blue) template structures, with the salt bridge between His264 and Glu169 broken (both residues' side chains shown as sticks), ECL3 tilted outward, and Glu169 directly interacting with the ligand (also shown as sticks). These conformational changes are far from what is sampled in either template simulation, indicating that the binding pocket conformation preferred by LUF5833 cannot be adopted in the subsequent FEP+ simulations.

12

ASSOCIATED CONTENT

Supporting Information.

Additional details on simulation setup and data analysis, including tables of results from all free energy calculations (PDF).

AUTHOR INFORMATION

Corresponding Author

*E-mail: lingle.wang@schrodinger.com; Phone: (212) 548-2381

Author Contributions

M.V. designed and performed research, analyzed data, and wrote the manuscript. B.W.Z. designed and performed research and edited the manuscript. J.K. designed research and edited the manuscript. L.W. designed research and edited the manuscript. All authors have given approval to the final version of the manuscript.

ABBREVIATIONS

MD, molecular dynamics; FEP, free energy perturbation; ABFEP, absolute binding FEP; RBFEP, relative binding FEP, ML, machine learning; LEP, ligand efficacy prediction; GPCR, G protein–coupled receptor; NR, nuclear receptor; OR, opioid receptor; RXR, retinoic acid receptor; IFD-MD, induced fit docking molecular dynamics; MCS, maximum common substructure; 5HT2A, serotonin receptor 2A, REST2, replica exchange with solute scaling; GCMC, Grand Canonical Monte Carlo.

REFERENCES

(1)   Dror, R. O.; Arlow, D. H.; Maragakis, P.; Mildorf, T. J.; Pan, A. C.; Xu, H.; Borhani, D. W.; Shaw, D. E. Activation Mechanism of the B2-Adrenergic Receptor. Proc. Natl. Acad. Sci. 2011, 108 (46), 18684–18689.

(2)   Kofuku, Y.; Ueda, T.; Okude, J.; Shiraishi, Y.; Kondo, K.; Maeda, M.; Tsujishita, H.; Shimada, I. Efficacy of the B2-Adrenergic Receptor Is Determined by Conformational Equilibrium in the Transmembrane Region. Nat. Commun. 2012, 3 (1), 1045.

(3)   Miao, Y.; McCammon, J. A. Graded Activation and Free Energy Landscapes of a Muscarinic G-Protein–Coupled Receptor. Proc. Natl. Acad. Sci. 2016, 113 (43), 12162–12167.

(4)   Fleetwood, O.; Matricon, P.; Carlsson, J.; Delemotte, L. Energy Landscapes Reveal Agonist Control of G Protein-Coupled Receptor Activation via Microswitches. Biochemistry 2020, 59 (7), 880–891.

(5)   Fleetwood, O.; Carlsson, J.; Delemotte, L. Identification of Ligand-Specific G Protein-Coupled Receptor States and Prediction of Downstream Efficacy via Data-Driven Modeling. eLife 2021, 10, e60715.

(6)   Dror, R. O.; Green, H. F.; Valant, C.; Borhani, D. W.; Valcourt, J. R.; Pan, A. C.; Arlow, D. H.; Canals, M.; Lane, J. R.; Rahmani, R.; Baell, J. B.; Sexton, P. M.; Christopoulos, A.; Shaw, D. E. Structural Basis for Modulation of a G-Protein-Coupled Receptor by Allosteric Drugs. Nature 2013, 503 (7475), 295–299.

(7)   Kruse, A. C.; Ring, A. M.; Manglik, A.; Hu, J.; Hu, K.; Eitel, K.; Hübner, H.; Pardon, E.; Valant, C.; Sexton, P. M.; Christopoulos, A.; Felder, C. C.; Gmeiner, P.; Steyaert, J.; Weis, W. I.; Garcia, K. C.; Wess, J.; Kobilka, B. K. Activation and Allosteric Modulation of a Muscarinic Acetylcholine Receptor. Nature 2013, 504 (7478), 101–106.

(8)   Wingler, L. M.; Skiba, M. A.; McMahon, C.; Staus, D. P.; Kleinhenz, A. L. W.; Suomivuori, C.-M.; Latorraca, N. R.; Dror, R. O.; Lefkowitz, R. J.; Kruse, A. C. Angiotensin and Biased Analogs Induce Structurally Distinct Active Conformations within a GPCR. Science 2020, 367 (6480), 888–892.

(9)   Powers, A. S.; Pham, V.; Burger, W. A. C.; Thompson, G.; Laloudakis, Y.; Barnes, N. W.; Sexton, P. M.; Paul, S. M.; Christopoulos, A.; Thal, D. M.; Felder, C. C.; Valant, C.; Dror, R. O. Structural Basis of Efficacy-Driven Ligand Selectivity at GPCRs. Nat. Chem. Biol. 2023.

(10)   Wang, L.; Wu, Y.; Deng, Y.; Kim, B.; Pierce, L.; Krilov, G.; Lupyan, D.; Robinson, S.; Dahlgren, M. K.; Greenwood, J.; Romero, D. L.; Masse, C.; Knight, J. L.; Steinbrecher, T.; Beuming, T.; Damm, W.; Harder, E.; Sherman, W.; Brewer, M.; Wester, R.; Murcko, M.; Frye, L.; Farid, R.; Lin, T.; Mobley, D. L.; Jorgensen, W. L.; Berne, B. J.; Friesner, R. A.; Abel, R. Accurate and Reliable Prediction of Relative Ligand Binding Potency in Prospective Drug Discovery by Way of a Modern Free-Energy Calculation Protocol and Force Field. J. Am. Chem. Soc. 2015, 137 (7), 2695–2703.

(11)   Wang, L.; Chambers, J.; Abel, R. Protein–Ligand Binding Free Energy Calculations with FEP+. In Biomolecular Simulations; Bonomi, M., Camilloni, C., Eds.; Methods in Molecular Biology; Springer New York: New York, NY, 2019; Vol. 2022, pp 201–232.

(12)   Chen, W.; Cui, D.; Jerome, S. V.; Michino, M.; Lenselink, E. B.; Huggins, D. J.; Beautrait, A.; Vendome, J.; Abel, R.; Friesner, R. A.; Wang, L. Enhancing Hit Discovery in Virtual Screening through Absolute Protein-Ligand Binding Free-Energy Calculations. J. Chem. Inf. Model. 2023, 63 (10), 3171–3185.

(13)   Bhattacharya, S.; Vaidehi, N. Computational Mapping of the Conformational Transitions in Agonist Selective Pathways of a G-Protein Coupled Receptor. J. Am. Chem. Soc. 2010, 132 (14), 5205–5214.

(14)   Kohlhoff, K. J.; Shukla, D.; Lawrenz, M.; Bowman, G. R.; Konerding, D. E.; Belov, D.; Altman, R. B.; Pande, V. S. Cloud-Based Simulations on Google Exacycle Reveal Ligand Modulation of GPCR Activation Pathways. Nat. Chem. 2014, 6 (1), 15–21.

(15)   Harpole, T. J.; Delemotte, L. Conformational Landscapes of Membrane Proteins Delineated by Enhanced Sampling Molecular Dynamics Simulations. Biochim. Biophys. Acta BBA - Biomembr. 2018, 1860 (4), 909–926.

(16)   Saleh, N.; Saladino, G.; Gervasio, F. L.; Clark, T. Investigating Allosteric Effects on the Functional Dynamics of B2-Adrenergic Ternary Complexes with Enhanced-Sampling Simulations. Chem. Sci. 2017, 8 (5), 4019–4026.

(17)   Panel, N.; Vo, D. D.; Kahlous, N. A.; Hübner, H.; Tiedt, S.; Matricon, P.; Pacalon, J.; Fleetwood, O.; Kampen, S.; Luttens, A.; Delemotte, L.; Kihlberg, J.; Gmeiner, P.; Carlsson, J. Design of Drug Efficacy Guided by Free Energy Simulations of the B2-Adrenoceptor. Angew. Chem. Int. Ed. 2022, 62 (22), e202218959.

(18)   Jespers, W.; Heitman, L. H.; IJzerman, A. P.; Sotelo, E.; Westen, G. J. P. van; Åqvist, J.; Gutiérrez-de-Terán, H. Deciphering Conformational Selectivity in the A2A Adenosine G Protein-Coupled Receptor by Free Energy Simulations. PLOS Comput. Biol. 2021, 17 (11), e1009152.

(19)   Scior, T.; Bender, A.; Tresadern, G.; Medina-Franco, J. L.; Martínez-Mayorga, K.; Langer, T.; Cuanalo-Contreras, K.; Agrafiotis, D. K. Recognizing Pitfalls in Virtual Screening: A Critical Review. J. Chem. Inf. Model. 2012, 52 (4), 867–881.

(20)   Hart, K. M.; Ho, C. M. W.; Dutta, S.; Gross, M. L.; Bowman, G. R. Modelling Proteins' Hidden Conformations to Predict Antibiotic Resistance. Nat. Commun. 2016, 7 (1), 12965.

(21)   Staus, D. P.; Strachan, R. T.; Manglik, A.; Pani, B.; Kahsai, A. W.; Kim, T. H.; Wingler, L. M.; Ahn, S.; Chatterjee, A.; Masoudi, A.; Kruse, A. C.; Pardon, E.; Steyaert, J.; Weis, W. I.; Prosser, R. S.; Kobilka, B. K.; Costa, T.; Lefkowitz, R. J. Allosteric Nanobodies Reveal the Dynamic Range and Diverse Mechanisms of G-Protein-Coupled Receptor Activation. Nature 2016, 535 (7612), 448–452.

(22)   Townshend, R.; Vögele, M.; Suriana, P.; Derry, A.; Powers, A.; Laloudakis, Y.; Balachandar, S.; Jing, B.; Anderson, B.; Eismann, S.; Kondor, R.; Altman, R.; Dror, R. ATOM3D: Tasks on Molecules in Three Dimensions. Proc. Neural Inf. Process. Syst. Track Datasets Benchmarks 2021, 1.

(23)   Wang, T.; Duan, Y. Ligand Entry and Exit Pathways in the B2-Adrenergic Receptor. J. Mol. Biol. 2009, 392 (4), 1102–1115.

(24)   Hurst, D. P.; Grossfield, A.; Lynch, D. L.; Feller, S.; Romo, T. D.; Gawrisch, K.; Pitman, M. C.; Reggio, P. H. A Lipid Pathway for Ligand Binding Is Necessary for a Cannabinoid G Protein-Coupled Receptor. J. Biol. Chem. 2010, 285 (23), 17954–17964.

(25)   Dror, R. O.; Pan, A. C.; Arlow, D. H.; Borhani, D. W.; Maragakis, P.; Shan, Y.; Xu, H.; Shaw, D. E. Pathway and Mechanism of Drug Binding to G-Protein-Coupled Receptors. Proc. Natl. Acad. Sci. 2011, 108 (32), 13118–13123.

(26)   Kruse, A. C.; Hu, J.; Pan, A. C.; Arlow, D. H.; Rosenbaum, D. M.; Rosemond, E.; Green, H. F.; Liu, T.; Chae, P. S.; Dror, R. O.; Shaw, D. E.; Weis, W. I.; Wess, J.; Kobilka, B. K. Structure and Dynamics of the M3 Muscarinic Acetylcholine Receptor. Nature 2012, 482 (7386), 552–556.

(27)   Copeland, R. A. The Drug–Target Residence Time Model: A 10-Year Retrospective. Nat. Rev. Drug Discov. 2016, 15 (2), 87–95.

(28)   Tonge, P. J. Drug–Target Kinetics in Drug Discovery. ACS Chem. Neurosci. 2018, 9 (1), 29–39.

(29) Santos, R.; Ursu, O.; Gaulton, A.; Bento, A. P.; Donadi, R. S.; Bologa, C. G.; Karlsson, A.; Al-Lazikani, B.; Hersey, A.; Oprea, T. I.; Overington, J. P. A Comprehensive Map of Molecular Drug Targets. Nat. Rev. Drug Discov. 2017, 16 (1), 19–34.

(30) Congreve, M.; Graaf, C. de; Swain, N. A.; Tate, C. G. Impact of GPCR Structures on Drug Discovery. Cell 2020, 181 (1), 81–91.

(31) Hu, Y.; Stumpfe, D.; Bajorath, J. Recent Advances in Scaffold Hopping. J. Med. Chem. 2017, 60 (4), 1238–1246.

(32) Wang, L.; Deng, Y.; Wu, Y.; Kim, B.; LeBard, D. N.; Wandschneider, D.; Beachy, M.; Friesner, R. A.; Abel, R. Accurate Modeling of Scaffold Hopping Transformations in Drug Discovery. J. Chem. Theory Comput. 2017, 13 (1), 42–54.

(33) Calderón, J. C.; Ibrahim, P.; Gobbo, D.; Gervasio, F. L.; Clark, T. General Metadynamics Protocol To Simulate Activation/Deactivation of Class A GPCRs: Proof of Principle for the Serotonin Receptor. J. Chem. Inf. Model. 2023, 63 (10), 3105–3117.

(34) Sala, D.; del Alamo, D.; Mchaourab, H. S.; Meiler, J. Modeling of Protein Conformational Changes with Rosetta Guided by Limited Experimental Data. Structure 2022, 30 (8), 1157-1168.e3.

(35) del Alamo, D.; Sala, D.; Mchaourab, H. S.; Meiler, J. Sampling Alternative Conformational States of Transporters and Receptors with AlphaFold2. eLife 2022, 11, e75751.

(36) Wayment-Steele, H. K.; Ovchinnikov, S.; Colwell, L.; Kern, D. Prediction of Multiple Conformational States by Combining Sequence Clustering with AlphaFold2. bioRxiv October 17, 2022, p 2022.10.17.512570. https://www.biorxiv.org/content/10.1101/2022.10.17.512570v1 (accessed 2023-04-24).

(37) Stein, R. A.; Mchaourab, H. S. SPEACH_AF: Sampling Protein Ensembles and Conformational Heterogeneity with Alphafold2. PLOS Comput. Biol. 2022, 18 (8), e1010483.

(38) Heo, L.; Feig, M. Multi-State Modeling of G-Protein Coupled Receptors at Experimental Accuracy. Proteins Struct. Funct. Bioinforma. 2022, 90 (11), 1873–1885.

(39) Sala, D.; Hildebrand, P. W.; Meiler, J. Biasing AlphaFold2 to Predict GPCRs and Kinases with User-Defined Functional or Structural Properties. Front. Mol. Biosci. 2023, 10, 1121962.

(40) Zhang, Y.; Vass, M.; Shi, D.; Abualrous, E.; Chambers, J. M.; Chopra, N.; Higgs, C.; Kasavajhala, K.; Li, H.; Nandekar, P.; Sato, H.; Miller, E. B.; Repasky, M. P.; Jerome, S. V. Benchmarking Refined and Unrefined AlphaFold2 Structures for Hit Discovery. J. Chem. Inf. Model. 2023, 63 (6), 1656–1667.

(41) Zhao, J.; Elgeti, M.; O'Brien, E.; Sar, C.; Daibani, A. E.; Heng, J.; Sun, X.; Che, T.; Hubbell, W. L.; Kobilka, B.; Chen, C. Conformational Dynamics of the μ-Opioid Receptor Determine Ligand Intrinsic Efficacy. bioRxiv April 29, 2023, p 2023.04.28.538657. https://www.biorxiv.org/content/10.1101/2023.04.28.538657v1 (accessed 2023-04-30).

(42) Dutta, S.; Shukla, D. Distinct Activation Mechanisms Regulate Subtype Selectivity of Cannabinoid Receptors. Commun. Biol. 2023, 6 (1), 1–16.

(43) Miller, E. B.; Murphy, R. B.; Sindhikara, D.; Borrelli, K. W.; Grisewood, M. J.; Ranalli, F.; Dixon, S. L.; Jerome, S.; Boyles, N. A.; Day, T.; Ghanakota, P.; Mondal, S.; Rafi, S. B.; Troast, D. M.; Abel, R.; Friesner, R. A. Reliable and Accurate Solution to the Induced Fit Docking Problem for Protein–Ligand Binding. J. Chem. Theory Comput. 2021, 17 (4), 2630–2639.

(44) Xu, T.; Zhu, K.; Beautrait, A.; Vendome, J.; Borrelli, K.; Abel, R.; Friesner, R.; Miller, E. Induced-Fit Docking Enables Accurate Free Energy Perturbation Calculations in Homology Models. ChemRxiv April 15,

2022. https://chemrxiv.org/engage/chemrxiv/article-details/6257731fbdc9c24981d3df0b (accessed 2023-04-30).

(45)   Harding, S. D.; Armstrong, J. F.; Faccenda, E.; Southan, C.; Alexander, S. P. H.; Davenport, A. P.; Pawson, A. J.; Spedding, M.; Davies, J. A.; NC-IUPHAR. The IUPHAR/BPS Guide to PHARMACOLOGY in 2022: Curating Pharmacology for COVID-19, Malaria and Antibacterials. Nucleic Acids Res. 2022, 50 (D1), D1282–D1294.

(46)   Vögele, M.; Thomson, N. J.; Truong, S. T.; McAvity, J.; Zachariae, U.; Dror, R. O. Systematic Analysis of Biomolecular Conformational Ensembles with PENSA. arXiv December 5, 2022. https://arxiv.org/abs/2212.02714v1 (accessed 2023-04-25).

(47)   Schrödinger Release 2023-1: FEP+, Schrödinger Inc., New York, 2023.

(48)   Wang, L.; Friesner, R. A.; Berne, B. J. Replica Exchange with Solute Scaling: A More Efficient Version of Replica Exchange with Solute Tempering (REST2). J. Phys. Chem. B 2011, 115 (30), 9431–9438.

(49)   Ross, G. A.; Russell, E.; Deng, Y.; Lu, C.; Harder, E. D.; Abel, R.; Wang, L. Enhancing Water Sampling in Free Energy Calculations with Grand Canonical Monte Carlo. J. Chem. Theory Comput. 2020, 16 (10), 6061–6076.

(50)   Rocklin, G. J.; Mobley, D. L.; Dill, K. A.; Hünenberger, P. H. Calculating the Binding Free Energies of Charged Species Based on Explicit-Solvent Simulations Employing Lattice-Sum Methods: An Accurate Correction Scheme for Electrostatic Finite-Size Effects. J. Chem. Phys. 2013, 139 (18), 184103.

(51)   Chen, W.; Deng, Y.; Russell, E.; Wu, Y.; Abel, R.; Wang, L. Accurate Calculation of Relative Binding Free Energies between Ligands with Different Net Charges. J. Chem. Theory Comput. 2018, 14 (12), 6346–6358.

(52)   Friesner, R. A.; Murphy, R. B.; Repasky, M. P.; Frye, L. L.; Greenwood, J. R.; Halgren, T. A.; Sanschagrin, P. C.; Mainz, D. T. Extra Precision Glide: Docking and Scoring Incorporating a Model of Hydrophobic Enclosure for Protein−Ligand Complexes. J. Med. Chem. 2006, 49 (21), 6177–6196.

(53)   Schrödinger Release 2023-1: Glide, Schrödinger Inc., New York, 2023.

(54)   Hunter, J. D. Matplotlib: A 2D Graphics Environment. Comput. Sci. Eng. 2007, 9 (3), 90–95.

(55)   The PyMOL Molecular Graphics System, Version 2.5.2, Schrödinger Inc., New York, 2022.

(56)   Schrödinger Release 2023-1: Maestro, Schrödinger Inc., New York, 2023.